FRACTURE CHARACTERIZATION BASED ON ORIENTED HORIZONTAL CORE FROM THE SPRABERRY TREND RESERVOIR: A CASE STUDY

Paul McDonald, Pioneer Natural Resources USA Inc.
John C. Lorenz, Sandia National Labs
Charlie Sizemore, Pioneer Natural Resources USA Inc.
David S. Schechter and Martha Cather, New Mexico PRRC
Tom Sheffield, Pioneer Natural Resources USA, Inc.

Introduction

Natural fractures existing over a regional area have long been known to dominate all aspects of performance in the Spraberry Trend Area[1]. However, there is little or no information on the actual fracture system other than: orientation, on a gross basis, from pulse and/or tracer tests in the 50's and 60's, and fracture spacing inferred from simulation and a few existing vertical cores. Previous descriptions and old core reports did not distinguish between natural and coring induced fractures, thus almost all information from the early years, when almost all Spraberry data was obtained, provides no detailed information on the natural fracture system. The first vertical core, taken as part of the current program in 1993 from the Shackelford Spraberry Unit #1-38A, intersected a vertical natural fracture with significant mineralization that had clearly grown into unoccupied space. This open, mineralized fracture was contained within a thin pay sand and was observed to terminate at a shale parting. This fracture was the first documented evidence of the existence of mineralized natural fractures within the pay sand.

The orientation, containment within zone, degree of mineralization, fracture aperture and spacing are important questions when considering fluid flow in naturally fractured reservoirs. However, after considerable data gathering, it became apparent that only superficial characterization of the natural fracture system was available. Recent acquisition of the horizontal core has radically altered understanding of the natural fracture system in the Spraberry Trend Area. This well, the E.T. O' Daniel #28, was cored with the intent of intersecting natural fractures in the thin sand streaks where oil saturation is found in the Upper Spraberry. Over 100 natural fractures were intersected from the 1U and 5U pay zones exhibiting an intriguing and diverse array of fracturing behavior. This paper describes the coring operation, fracture analysis of the cores and log analysis from the horizontal wellbore.

Acquisition of Horizontal Cores from the Dual Lateral E.T. O'Daniel #28

The Spraberry formation was deposited during the Permian age within the Leonardian system in the Midland Basin, a part of the province known as the Permian Basin of West Texas and Southeast New Mexico. The depositional environment consisted of a combination of turbidity and density currents sourced from the northwestern shelf area. The Spraberry formation facies can be characterized as submarine fan and basin plane deposits and consists of very fine grained sandstones to coarse grained siltstones and mudstones. The various fan complexes can be traced to the north in Dawson and Lynn counties and are considered the source material for the fan lobe sequences within the area of study in eastern Midland County.

Since its discovery, the Spraberry has been subdivided into three principal intervals, the lower, middle and upper Spraberry formations. In the late 1980's, Tyler and Gholston further subdivided the Spraberry intervals to represent distinct episodes, or operational units, within each of the submarine fan complexes (Fig. 1)[2]. Six of these units were found in the Upper Spraberry and two in the Lower Spraberry. Only two of the six horizons in the Upper Spraberry (1U and 5U) have been identified as containing reservoir quality rock capable of making significant production contributions.

The proposed target of the horizontal core was the natural fractures within the main pay intervals of the 1U and 5U sands. Net pay within each of these zones averages between 8 and 14 ft. depending on location. Unfortunately, logs run following the coring of the 1U interval confirmed that the core had actually come from a thinner (2-3 ft.) pay section, within the 1U interval, located 6-8 ft. above the main pay.

One of the primary objectives in obtaining horizontal core was to provide direct measurement of fracture orientation and spacing, therefore, the well plan called for both laterals to extend perpendicular to the assumed fracture trend in order to maximize the intersection of natural fractures. The mechanics of obtaining the core in a horizontal well proved to be not unlike that of coring a vertical well. In fact, the problems which hampered horizontal coring operations were typical of problems commonly encountered in coring vertical wells.

Curve Build Bottom Hole Assembly. The bottom hole assembly (BHA) utilized to drill the curve on both the Upper Spraberry 1U and 5U targets was as follows: 6-1/2" PDC bit, 5" O.D., 5/6 lobe 4 stage adjustable angle motor, flex sub, float sub with stainless steel insert float, UBHO (Universal Bottom Hole Orienting) sub, and 2 non-magnetic monel drill collars. The BHA was run on 3-1/2" IF drill pipe.

Coring Bottom Hole Assembly. The first BHA utilized to perform the coring operations was configured as follows: 6-1/8" diamond core bit, 6-1/8" O. D. scribe shoe with slip dog core catcher, 6-1/8" X 2-5/8" X 30' core barrel with aluminum inner barrel, 4-3/4" O. D. monel drill collar with electromagnetic survey (EMS) tool inside, and 2 monel drill collars (Fig. 2). The core bit was threaded onto the outer core barrel and was rotated by the power swivel at the surface. The inner barrel, located inside the outer barrel, was allowed to rotate independently through a bearing pack assembly. The scribe shoe, which has three scribe knives in a symmetrical position around the circumference of the shoe, was threaded onto the bottom of the inner barrel. The knives are used to keep the barrel from rotating with the outer barrel. The other function of the knives is to scribe the core with orientation lines as the core enters through the shoe into the inner barrel. The entire assembly was run in the hole on 3-1/2" IF drill pipe. After core run #1 in the 5U sand failed, the bit design was changed from a standard diamond design to a 6-1/8" X 2-5/8" PDC design. One monel collar was dropped from the drill string. After core run #4 in the 5U sand , the core catcher assembly was strengthened by adding a basket catcher and a split ring catcher. The basket catcher was dropped from the assembly after core run #5.

Orientation Tool And Procedure. The electronic survey instrument chosen to orient the recovered core is a three axis system utilizing accelerometers and magnetometers to determine well bore inclination, well bore direction, and core barrel scribe knife orientation. Information obtained from the survey is stored in memory and downloaded at the surface after each core run. The tool is capable of storing over 7,700 readings, has no attitude or heading limitations, and is programmable over a wide range of timing intervals, allowing for greater flexibility. The orientation assembly consists of an instrument pressure barrel, rotating centralizers, and spacer bars to correctly space the tool inside the non-magnetic drill collar (Fig. 2). The survey instrument is calibrated electronically prior to its arrival on location.

Core barrel alignment is accomplished by placing an orientation mark on the assembly distinguishing the high side of the survey instrument and aligning it to the main scribe knife in the scribe shoe. To accomplish this, the outer barrel is suspended at the surface by the rig blocks. The inner barrel is then removed and a protractor is aligned with the main scribe knife. The inner barrel is then lowered and a mark is placed on an orientation rod attached to the top of the inner barrel. The survey instrument is threaded onto the orientation rod, the marks on the rod and the instrument assembly are aligned, and the tool is set in place through the use of set screws. The core barrel assembly is then screwed back together and run in the hole.

Well Plan And Coring Proposal. The well plan called for a curve with a dogleg severity (DLS) of less than 19°/100 ft. to minimize deflection of the core. A radius of curvature of 400 ft., providing a DLS of 14.32° /100 ft. was chosen to optimize drilling time and to allow maximum flexibility. The proposed hole diameter of the curve was 6-1/2" O. D. to increase tool string mobility if the DLS became critical. Planned weight on bit (WOB) was from 3,000 lbs. to 5,000 lbs. Rotary speeds were to operate in the range of 35 RPM minimum to a maximum of 65 RPM.

The Upper Spraberry 5U casing exit called for a section cut from 6,788' to 6,858' with a proposed kick off point (KOP) of 6,838'. The true vertical depth (TVD) of the 5U target was projected to be 7,238' TVD. The Upper Spraberry 1U casing exit called for a section cut from 6,639' to 6,709' with a proposed KOP of 6,689'. The 1U target was projected to be 7,089' TVD.

Original plans were to cut and retrieve 150 ft. of 2-5/8" diameter oriented core from each zone in 30 ft. increments. Clean out and TVD correction runs were to be performed as needed, based upon core recovery and mud log information.

Upper Spraberry 5U Casing Exit and Curve Summary. A 7- 5/8" cast iron bridge plug (CIBP) was run in the hole via electric wireline and set at a depth of 6,890 ft. A 75 ft. section of the 7-5/8" casing from 6,788 ft. to 6,863 ft. was then milled out using a 7-5/8" section mill. A caliper log was run across the interval to verify the actual amount of casing removed. For the cement kick off plug, a slurry of class "C" w/1% $CaCl_2$ was pumped and allowed to set for 24 hours to attain sufficient compressive strength for kick off. The plug was then tagged with the drill string to locate the top of cement. Upon tagging the plug, the top was found below the proposed KOP, necessitating pumping a second plug. After another 24 hour curing period, the plug was tagged and dressed off to the KOP of 6,838 ft.

The curve build BHA was made up on the surface and run in the hole to the KOP. Circulation was established with a fluid rate of 50 gallons per minute (gpm) and an air rate of 150 gallons per minute equivalent (gpm eq.) at the motor. The build section was drilled on an azimuth of 167 degrees from 6,838 ft. measured depth (MD) to 7,488 ft. MD resulting in a radius of curvature of 414 ft. with a DLS of 13.85 degrees/100 ft.

Upper Spraberry 5U Coring Summary. The first coring assembly was made up on the surface and run in the hole to the KOP. Circulation was established with the foamed air/brine mixture, the assembly was run to bottom, and coring operations were initiated.

The Upper Spraberry 5U sand was cored and drilled from 7,488 ft. MD to 7,931 ft. MD for a total of 443 ft. with a net core recovery of 169 ft. (Fig. 3). Core run #1 resulted in zero ecovery and an extremely low ROP of 35.3 min./ft. The bit design was changed from a standard diamond core bit to a 6-1/8" X 2-5/8" PDC design, increasing ROP tremendously. Core runs #2 and #3 resulted in 58 ft. of core recovery. Core run #4 was successful but the core was lost when the core catcher assembly failed at the surface during breakdown procedures. The catcher design was changed from a single slip dog catcher to a triple assembly consisting of a slip dog catcher, a basket catcher, and a split ring catcher. Core run #5 resulted in a 20 ft. recovery. Determining that the catcher assembly was too conservative, the basket catcher was dropped for subsequent core runs. Core run #6 resulted in only 6 in. of recovery due to rubble in the hole. After a clean up run, core runs #7 - #9 resulted in 89.5 ft. of recovery which terminated coring operations in the 5U.

Upper Spraberry 1U Casing Exit and Curve Summary. A 7- 5/8" retrievable bridge plug (RBP) was run in the hole via electric wireline to a depth of 6,750 ft. but set unsuccessfully. The plug and setting tool were removed from the hole and a second plug was successfully set at 6,750 ft. with two sacks of sand on top of the plug. A 30 ft. section of the 7-5/8" casing from 6,609 ft. to 6,639 ft. was milled out using a 7-5/8" section mill. A caliper log was then run across the milled interval to verify the actual amount of casing removed. For the cement kick off plug, a slurry of class "C" w/1% $CaCl_2$ was pumped and allowed to set for 24 hours to attain sufficient compressive strength for kick off. The plug was then tagged with the drill string to locate the top of cement. Upon tagging the plug, the top was found below the proposed KOP, necessitating pumping a second plug. After another 24 hour curing period, the plug was tagged and dressed off to the KOP of 6,612 ft.

The curve build BHA was made up on the surface and run in the hole to the KOP. Circulation was established with a fluid rate of 50 gpm and an air rate of 140 gpm eq. at the motor. The build section was drilled on an azimuth of 157.7 degrees from 6,612 ft. MD to 7,330 ft. MD resulting in a radius of curvature of 457 ft. with a DLS of 12.53°/100 ft.

Upper Spraberry 1U Coring Summary. The coring assembly consisting of a 6-1/8" X 2-5/8" PDC bit, scribe shoe with slip dog and split ring catchers, 6-1/8" X 2-5/8" X 30' core barrel with aluminum inner barrel, 4-3/4" monel drill collar with EMS survey tool, 4-3/4" monel collar, and crossover sub was made up and run in the hole on 3-1/2" IF drill pipe to the KOP. Circulation was established with the foamed air/brine mixture, the assembly was run to bottom, and coring operations were initiated.

The Upper Spraberry 1U sand was cored and drilled from 7,330 ft. MD to 7,727 ft. MD for a total of 397 ft. with a net core recovery of 226 ft. (Fig. 3). Core runs #1 and #2 resulted in net core recovery of 62 ft. Core run #3 resulted in net recovery of 8 ft. before the core barrel jammed with black shale, indicating that the well path was out of zone. After a clean out and TVD correction run, core runs #4 - #8 resulted in a net recovery of 153 ft. Core run #9 resulted in a net recovery of 3 ft. before the barrel jammed and coring operations were terminated.

Fracture Analysis of the E.T. O'Daniel #28 Horizontal Core

Three distinct fracture sets, trending NNE, NE, and ENE, are present in cores from the 1U and 5U reservoirs.[3] NE fractures are commonly mineralized with barite and are found only in the 1U reservoir. Unmineralized NNE and ENE fractures occur in the 5U reservoir. Unmineralized ENE fractures are also more widely distributed within the black shales overlying both the 1U and 5U reservoirs, and locally near the top of the 1U unit. However, no fractures are present in the black shales underlying either reservoir. Each fracture set has its own characteristic and distinct patterns of 1) spacing, 2) mineralization, 3) distribution with respect to lithology, 4) surface characteristics, and 5) distribution of strikes. Therefore each fracture set is most likely to have resulted from a separate stress event. Aspects of these fractures that are important to production are as follows: 1) fracture strikes are segregated by reservoir unit 2) NE fractures are typically partially mineralized, but mineralization is absent in this set at the base of the 1U reservoir 3) none of the NNE or ENE fractures are mineralized 4) no fractures are present in the shales underlying both reservoirs, but ENE fractures occur in shales overlying both reservoirs.

Orientation. Three distinct natural fracture orientations are present in these horizontal cores, trending approximately NNE, NE, and ENE (Table 1).

Although the total range of strikes for each fracture set is about 25 degrees, the distribution of those strikes varies by set (Figs. 4 and 5). Most of the NE fractures occur within a narrow range (5 degrees) of distribution while most of the ENE fractures fall within a somewhat broader (20 degree) distribution of strikes. The ENE fracture strikes are relatively scattered within the total range of nearly 30 degrees.

Stratigraphic and Lithologic Controls. All 28 NNE fractures occur within the 5U reservoir, while the entire set of 46 NE-striking fractures is contained within the 1U reservoir. Fractures of the ENE fracture are not confined to either the 5U reservoir or to the sandy facies of either reservoir, although they are more common in the 5U unit. Eleven of the ENE fractures are present within the good 5U reservoir facies, seven ENE fractures are present near the top of the 1U reservoir in silty zones of poor florescence, and eleven more ENE fractures are present in the black shale facies overlying both the 1U and 5U reservoirs. No fractures of any set are present in any of the long cores taken from the black shale facies below either reservoir.

Spacing. The NNE fractures are very closely spaced. The average ENE fracture spacing is significantly larger, more than double that of the NNE fractures. NE fractures also have a wide average spacing similar to that of the ENE fractures (Table 2).

Each fracture set has a distinct pattern to its spacing distribution. The spacing distribution for the NNE fracture set (Fig. 6) conforms to the log-normal pattern typical of regional fractures; i.e., numerous closely spaced fractures and fewer widely spaced fractures. The ENE fracture set (Fig. 6) has somewhat fewer of the fractures spaced less than one foot apart, but has a significant number of fractures within the one foot to three foot range. These ENE fractures are widely and irregularly scattered throughout the Spraberry formation, and the tail on the ENE fracture distribution histogram is significantly longer than that for either the NNE or NE sets, extending to 13 feet (Fig. 6).

In contrast, the NE fracture set is relatively regularly spaced (Fig. 6). The spacing distribution histogram for the NE fracture set shows relatively few and nearly equal numbers of both closely and widely spaced fractures, a narrow range of spacings, and a dominance of intermediate spacings of one to four feet. This fracture set is much more evenly distributed within the formation than either of the other two sets, or than is typical of regional fractures.

Apertures, Mineralization, and Surface Characteristics. Only fractures of the NE striking set (and thus only fractures in the 1U reservoir) contain obvious mineralization. This mineralization is inferred to be barite, and varies in extent from complete filling of original fracture apertures less than a millimeter wide to a complete absence of mineralization along hairline cracks in the intact rock. Most of the fractures of this set contain some mineralization with the average percentage of filling being on the order of 75%. Where fractures are incompletely mineralized, patches of barite with local crystal faces and rosettes are common, indicating open porosity and permeability pathways at depth. Most of the unmineralized NE fractures occur near the base of the 1U reservoir. This relationship is consistent in both intervals where the base of the 1U was cored. Although the reason for this local absence of mineralization is presently unclear, it may be related to local geochemical environments caused by segregation of hydrocarbons and formation waters.

In contrast, none of the ENE or NNE fractures contain mineralization, even in those few intervals where they occur in conjunction with mineralized NE fractures. Rather, the ENE and NNE fractures have gray or brown-stained surfaces that are distinct from the fresh, irregular, coring-induced breaks in the rock. Microscopic crystalline overgrowths may be present on some of the sand grains lining these surfaces.

The ENE fracture surfaces tend to be planar and smooth, whereas many of the NNE fractures occur as anastomosed or en echelon fracture segments with rough fracture surfaces and mm-scale en echelon fracture offsets. Preferred trend to the en echelon steps suggest incipient right-lateral shear.

The NNE and ENE fractures appear as hairline cracks in the core surface where the core has remained intact across the fracture surfaces. This is suggestive of significant in situ conductivity capability along the fractures.

Possible Fracture Origins. The average strikes of the NNE and ENE fractures are respectively 11 degrees counterclockwise and 27 degrees clockwise from the average strike of the NE fracture set. This initially suggests that these three fracture sets might be interpretable as 1) a conjugate pair (the NNE and ENE fracture sets), with 2) a related NE fracture set sub-parallel to the bisector of the acute angle between the conjugate pair. Relatively small changes in stress conditions between the two reservoir units and/or subtle differences in the mechanical properties of the two units would have sufficed to create parallel vertical extension fractures in one bed and a related conjugate pair in the other bed.

However, in addition to the fact that the NE set does not precisely bisect the strike angle between the other two sets, there are several arguments against this interpretation:

Only the NNE set of the supposed NNE-ENE conjugate pair shows signs of the shear stress (the en echelon steps and offsets) that should accompany conjugate fracturing. The ENE half of the pair occurs throughout the formation (except in the shales below the reservoirs), and commonly as the only fracture set present, rather than being limited in distribution to an association with the NNE half of the pair. The ENE fractures show no indications of a shear stress origin. The NE set of fractures is mineralized whereas the other two sets are not: this suggests that the NE fracture set had formed and was mineralized prior to the formation of the other two sets under non-mineralizing conditions. Each of the three fracture sets has its own distinguishing characteristics (including unique spacing and orientation distributions, surface characteristics, and distributions with respect to lithology), which separate the fracture sets and suggest that each formed under a different condition of stress and/or lithification. One, albeit ambiguous, intersection between fractures of two sets was cored, this intersection suggesting that a NNE fracture terminates against, and is therefore younger than, an ENE fracture, rather than being part of a contemporaneous pair.

The conjugate sets theory is simple and clean and it has not been abandoned entirely, but it seems untenable based on these observations. An alternative but somewhat cumbersome interpretation is to suggest three separate fracture events, with the mineralized NE fractures being oldest, the ENE fractures of intermediate relative age, and the NNE fractures youngest. If the stress orientations have not changed since the formation of the youngest fractures, the maximum horizontal in situ compressive stress should then, theoretically, parallel the youngest fracture set. While this interpretation seems uncomfortably complex for this deep basin area of minimal structure, it would seem to best explain the data as presently understood.

Correlation of Core Fractures to Wellbore Image Log. A wellbore image log was run in the horizontal hole along the upper 1U interval. Although the images seem to be of good quality, there is an unsettling ambiguity in the correlation of log and core fractures (Fig. 7).

In order to analyze this ambiguity, a six inch tolerance was used (i.e., an imaged fracture is assumed to correlate to a fracture in core if it is within plus or minus six inches of the measured core depth), and only the intervals where both core and log data are available were considered. In this interval, there are 24 fractures in core that have no correlative fractures at the equivalent depth in the image log, and 36 fractures in the image log that have no equivalents in the core. A maximum of only 15 fractures are definitively present in both the core and the image log, no matter what depth shifts are applied. Fracture swarms and isolated fractures in core, which should have made easily recognizable patterns in the image log and thus provided good core-log tie points, have not left similarly-obvious patterns on the image log.

Nevertheless, the overall fracture strike trend indicated by the image log is nearly aligned with the average of the fracture orientations measured in core. The secondary trend of ENE fractures in the core is also present in the image log, within the approximately correct measured-depth intervals.

The reasons for agreement in strike without a one-to-one correlation of individual fractures are unclear. Stretch during conveyance of the imaging tool and the common depth ambiguity of cores make exact depth determinations difficult and may explain some of the discrepancy. However these factors can not account for the significant over count of fractures (133%) made by the image log relative to the natural fractures in core. It has been suggested that the log is seeing fractures that were missed by the naked eye during minute core examination (unlikely, and which moreover would be insignificant to production if present). However, the images on the log do not indicate that any of the fracture apertures are significantly less than others. Coring induced fractures that formed in the wellbore but not in the core might also explain the apparent over count, but with the present images it is not possible to distinguish these from natural fractures. Moreover, this would not account for the mineralized fractures that are present in the core but not apparent in the image log.

In general, the patterns of fracture positions and the numbers of fractures in the core and image log are not compatible, although the average fracture strikes are. This suggests that image logs should be calibrated with core wherever possible.

Fracture Diagenesis

During the past several months, work has continued on characterizing fractures at the microscopic scale by means of thin section petrography, electron microprobe analysis, and scanning electron microscopy. Work done so far seems to confirm the early conclusion that there are indeed three distinct fracture sets, and it is possible to speculate on the relationships between these three sets.

1U Fractures. Microscopic examination of 1U fracture surfaces shows that barite occurs as large crystals, up to a millimeter or more in size, with very smooth tabular faces. Barite crystals can partly to completely cover the surfaces of 1U fractures and appears to occlude porosity and may be responsible for reducing the crossflow of fluids and gas between rock matrix and fracture porosity (Figs. 8 and 9).

Quartz and dolomite occur in varying abundance as authigenic minerals on 1U fracture surfaces, however their size and morphology do not seem to have the same deleterious effect on porosity. Crystal sizes of quartz and dolomite are generally commensurate with the sizes of quartz and dolomite grains within the rock matrix, about 50 microns or less for quartz and generally less than 10 microns for dolomite. Thus, they do not appear to grow over and cover pore space that connects matrix with fracture (Fig. 10). Indeed, although quartz crystals seem insignificant in terms of abundance and size, they provide numerous asperities that may prevent fractures from closing even at reservoir pressure conditions (Fig. 11). The presence of abundant euhedrally-terminated quartz crystals demonstrates that fractures were open during certain periods of diagenesis.

In 1U fractures, it is apparent that fractures formed after early-stage diagenesis and dolomitization of carbonate grains and mud, but are syngenetic with some quartz precipitation and precipitation of ferroan dolomite, as both of these phases occur within matrix and within the fractures. Barite was not seen anywhere except in fractures, indicating precipitation later in the diagenetic history of the Spraberry.

5U Fractures. Closer examination of 5U fractures shows that surface mineralization is present on these fractures, but not in the same abundance as in 1U fractures. Quartz and dolomite are both fairly common, but barite is rare. As in the 1U, crystal size and habit of both quartz and dolomite are commensurate with their grain sizes in the host matrix, and the mineralization probably has no adverse effect on permeability between rock matrix and fracture porosity (Figs. 12 and 13). Barite occurs as large crystals up to 1 mm in diameter, similar to the 1U. But its scarcity within the 5U, at least in this horizontal core, makes it relatively unimportant as a possible fracture seal. Barite was observed in a few 5U samples as large crystals within the rock matrix near fractures. It appears to be a pore-filling cement. Because of the large crystal size, it is suspected that it has either replaced some detrital constituent of the siltstone or is filling vacancies caused by dissolution of some precursor grains and cements, possibly detrital and authigenic carbonates.

One cement type that was not seen in 1U fractures but that was seen in several 5U fractures of N70E orientation was calcite (Fig. 14). SEM examination showed that calcite-encrusted surfaces tended to be somewhat rough and in some cases striation son surfaces were seen. Because the striations are in a variety of orientations, it is probable that they were caused by dissolution along twin plane lamellae in calcite, rather than by mechanical scratching from movement of various matrix blocks relative to each other. Few crystals showed good euhedral terminations (Fig. 15). This may be due either to dissolution, or may indicate the lack of a significant amount of void space within fractures during crystal growth. An unmineralized N32E fracture was found in one sample to terminate against a calcite-filled N70E fracture, indicating later formation for the N32E-trending fracture set. Calcite-filled fractures are also found in unoriented middle Spraberry cores from other vertical wells drilled in the area. It is possible that the NNE fracture set of the 5U is related to some fracture event that had a locus of activity within the middle Spraberry, or it may be that proximity to the carbonate-rich middle Spraberry enabled calcite precipitation only within lower parts of the upper Spraberry.

Effects Of Matrix Composition On Fracxtures. Measurements of grain size and detrital composition were made in both 1U and 5U samples to see if there was any affect of these factors on fracture distribution or mineralization. Additionally, we wanted to see if fracture mineralization had changed the rock matrix composition by dissolution or precipitation of additional cements. This work is still underway, but preliminary results suggest that there is no relationship between fracture distribution with either grain size or detrital composition. Within the 5U samples, there is locally more calcite cement in the rock matrix adjacent to the calcite-filled fractures. Calcite is relatively uncommon in most Spraberry siltstones, and most carbonate is dolomite, ferroan dolomite, or ankerite. Therefore in at least a few instances, fracture diagenesis has altered the nearby rock matrix composition.

Paragenetic Sequences. Table 3 shows a summary of the paragenetic sequences for 1U and 5U fractures. In the 1U, fracturing is fairly straightforward. The N42E fracture set probably occurred first, as there is no barite mineralization within the few N80E fractures that were noted. Following fracturing, minor dolomite and quartz precipitation occurred. There is no clear indication which mineral phase precipitated first. Based on preliminary scanning cathodoluminescence studies (CL), it is believed that these cements were being precipitated both within the rock matrix and the fractures themselves contemporaneously. The barite was formed at a later time, shown by the fact that there is little or not barite noted in the rock matrix.

5U fracture paragenesis is more complicated, as there are two sets of fractures. It is believed that the N70E fracture set formed first, as there are a couple of examples of these fractures causing termination of N32E fractures. As in the 1U, diagenesis of matrix and fracture probably occurred near the same time. Later movement of fluids through the fractures caused at least local precipitation of calcite within fractures and nearby rock matrix. Evidence of some dissolution of calcite crystals within fractures demonstrates continued movement of fluid through fractures. The N32E fracture set formed subsequent to the first fracture event. There is minor precipitation of quartz and dolomite within the N32E fractures. Barite precipitation probably occurred following the first fracture event, but there is not enough evidence to determine its relation to the second fracture event. The fact that it is not abundant in any 5U fractures and was noted on fracture surfaces only in samples containing N70E fractures suggests that it probably occurred between the two events.

A possible sequence of events is shown in Fig. 16. The earliest stages of diagenesis and dolomitization were followed by a period of fracturing, possibly the N70E fracture set in the 5U. The stresses or events causing these fractures may have been stronger deeper within the Spraberry, as suggested by the presence of calcite-filled fractures within the middle Spraberry and the 5U but not within the 1U. Precipitation of calcite cement within the N70E fractures followed. The next event was probably fracturing within the 1U that caused the N42E fractures. At least three phases of carbonate are present in some 1U samples, with dolomite being the first-formed phase followed by ankerite, then a ferroan dolomite (see Fig. 9). Ferroan dolomite is the most common phase seen within the 1U fractures. Non-luminescent quartz cement is seen both within fractures and rock matrix, suggesting that fracturing and precipitation of quartz and ferroan dolomite were occurring at the same time. Precipitation of barite within 1U fractures and possibly within the 4U followed. A third fracture event then affected the 5U and formed the N32E fractures. This event was the only that involved any obvious signs of incipient shear stress; the other fractures are solely tension-type fractures. Precipitation of quartz and dolomite within this fracture set then followed.

Application of Rock-Log Model to the Horizontal Core Well

A schematic diagram of the two horizontal cores from the E.T. O'Daniel #28 well in shown in Fig. 17 (not to scale). Figure 18 summarizes fracture characteristics noted in the two horizontal cores from both pay and non-pay lithologies.

Figure 19 shows the open-hole logs from the E.T.O'Daniel # 28 horizontal well (Upper Spraberry). The volume of shale was calculated from gamma ray (GR) logs using the Larionov non-linear relationship. Effective porosity was calculated from the bulk-density log and integrated with whole core porosity.

As previously mentioned, there is evidence indicating that the upper cored interval of the O'Daniel #28 horizontal well is not actually the main 1U pay zone, but is one of the two thin pay sands that immediately overlie this zone (Fig. 17). A detailed comparison of gamma logs from the vertical log of this well and the log that was made from the horizontal redrilling shows that there is good correspondence of gamma peaks between the two logs (Fig. 20). As the horizontal well begins its curve from vertical to horizontal, the depths do not correspond, and the gamma peaks in the horizontal log become broader and less sharp as the log reflects the increasing curvature of the hole. Still, peaks have a good one-to-one correspondence, and the peak that constitutes the major Spraberry sand encountered in the horizontal core does not correspond to the main pay zone of the 1U, but to the second small sand that is encountered *above* the 1U. A similar relationship can be seen when examining the lithodensity log. Dolomite zones, corresponding to intervals of high bulk density, can be compared. Again, the main "pay" interval is actually above the true 1U. We were unable to log the 5U lateral due to the continual problem of tools getting jammed in the 5U curve.

Examination of the lithodensity-neutron crossover log provides further confirmation (Fig. 21). Within the logged interval, there are only three zones of crossover. The first is small and occurs at a log depth of 7250 ft. The second zone of crossover is thicker, from 7360 ft to 7400 ft, and this corresponds to the second sand above the 1U. This is the zone that was cored. Based on the hole geometry, the sand interval is only about three feet thick, much thinner than the pay zone interval (10 ft) of the 1U sand as determined from application of the rock-log model to the vertical log.

A fourth line of evidence supporting the argument that the primary 1U pay zone was not actually cored in the horizontal drilling operation is the close correlation between the core description and the well log after depth correction. At the top of core #1, 7330 ft core depth and 7315 ft log depth, there is a 25-ft interval of non-pay, non-fluorescing material. At a depth of 7355 ft (7340 ft log depth) sand percentage begins to increase and the core has poorly developed fluorescence. This trend continues and corresponds with the decrease in gamma count and a decrease in percent dolomite. At a measured depth of 7380 ft (7365 ft core depth), good fluorescence and the lowest gamma and bulk density readings are encountered. This corresponds to the gamma low of the second thin sand above the main 1U pay zone. At a core depth of 7425 ft, a sharp contact between fluorescing and non-fluorescing zones is encountered, again corresponding to the higher gamma counts seen in the well log, which indicate a zone of increased shale content.

The horizontal core well penetrated the two sand stringers that overlie the true main 1U pay zone. The reasonable production rates from this 3-ft thick zone are puzzling. The well has produced water-free oil for several months, which is rare in a 40 year old waterflood unit. There are two possible explanations. One explanation may be that the various sands within the 1U are not in direct communication with each other. No natural fractures were seen in the shaley zones below the cored sand; however, other fractures from other cores do show continuity of fractures through small zones of lithologic change, and it could be that such fractures were simply not encountered in the small section of core that was taken from between the shale overlying the main 1U pay zone (Fig. 18). Another possibility may be that production is controlled by fracture intensity, and fracture density is higher within thinner competent beds than in the thicker beds.

Also, crossplots of gamma ray vs. shale volume indicate that there is very little of the pay sand classified as rock type A, based on the our rock-log model[1] (Fig. 22). It can be observed from the Fig. 22 that cut-off criteria previously developed from vertical well logs can accurately quantify rock type in the horizontal well. Data points, where the volume of shale is less than 15% and the effective porosity is greater than 7% (Rock Type A) are sandiest part of the second sand above the 1U unit. Data points, where the volume of shale is less than 15% and the effective porosity is less than 7% (Rock Type B) are from the marginal pay of the 1U sequence. Core data indicates these zones are marginal pay. The porosity of these zones is drastically reduced due to presence of dolomite cement. Data points, where the volume of shale is greater than 15%, are from muddy non-pay zones of the Upper Spraberry as the horizontal wellbore traverses shale zones (Rock Type C). Most data points from the 1U horizontal cores lie either in regions B (marginal pay) or C (nonpay), atypical of reservoir rock from the main 1U pay.

The Upper Spraberry 1U sand was drilled and cored from 7,330 ft. MD to 7,727 ft. MD for a total of 397 ft. with a net core recovery of 226 ft. Core runs #1 and #2 resulted in net core recovery of 62 ft. Core run # 3 resulted in net recovery of 8 ft. before the core barrel jammed with black shale, indicating that the well path was out of zone. After a clean out and TVD correction run, core runs #4 - #8 resulted in a net recovery of 153 ft. Core run #9 resulted in a net recovery of 3 ft. before the barrel jammed and coring operations were terminated[2]. Core runs #1 & #2 are from 7,330-7,390 ft. Core runs #3 & #4 are from 7,390-7,430 ft. Core runs #5 & #6 are from 7,587-7,643 ft. Core runs #7 & #8 are from 7,662-7,693 ft. and Core run #9 are from 7,722-7,726 ft.

Core analysis of these cores were performed by Reservoirs Inc. A surface gamma ray log of the each core was recorded for downhole correlation. Full diameter ultraviolet and natural photographs were taken for permanent record. Water and oil saturations were determined by Dean-Stark Extraction. Porosity was determined using Boyle's law. Horizontal and vertical permeability to air was measured using the Hassler Sleeve Permeameter. Comparison of these cores are shown in Table 4.

Verification of Rock-Log Model. Integration of core and log data indicates that cut-off criteria for log-based Rock Type A are similar to the rock properties observed in core runs #3 & #4 and #7 & #8. Though these core runs are from the second sand above the main 1U pay zones, the high quality of these rocks are due to the horizontal direction of bedding plane and considered as pay. Cut-off criteria for log-based Rock Type B are similar to the core runs #1 & #2 and #9, which are considered as non pay. Cut-off criteria for the log-based Rock Type C are observed in core runs #5 & #6, which are non-pay muddy zones. These core observations of oil saturation in porosities greater than 7% verify the rock-log model developed based on vertical wells.

Conclusion

1. Acquisition and orientation of the horizontal core was a mechanical success. Drilling procedures, in fact, proved to be not unlike that of coring a vertical well.
2. Acquisition of this core unequivocally documents numerous, closely spaced natural fractures in the reservoirs of the Spraberry formation and led to the following major conclusions: 1) Three distinct fracture sets, trending NNE, NE, and ENE, are present in the cores from the 1U and 5U reservoirs. NE fractures are commonly mineralized with barite and are found only in the 1U reservoir. Unmineralized NNE and ENE fractures occur in the 5U reservoir. 2) Each fracture set has its distinct pattern of spacing, mineralization, distribution with respect to lithology, surface characteristics and distribution of strikes. Therefore each fracture set is most likely to have resulted from a separate stress event. 3) There was an unsettling ambiguity in the correlation of the fractures found in the core and the fractures found on the well bore image log. Orientation of the fracture sets from the core and logs were similar, however, there was a significant over count (133%) of fractures made by the image log relative to the natural fractures in the core.
3. The rock-log model, previously developed from open and cased-hole logs from vertical wells can be applied successfully to the new horizontal well drilled in the Spraberry Trend and can be used successfully for placement of horizontal wells within thin pay sands.

References

1. Schechter, D.S.: "Advanced Reservoir Characterization and Evaluation of CO_2 Gravity Drainage in the Naturally Fractured Spraberry Trend Area," First Annual Technical Progress Report, Contract No. DE-FC22-95BC14942, U.S. DOE (Dec 1996).
2. Tyler, N., and Gholston, J.C.: "Heterogeneous Deep-Sea Fan Reservoir, Shackelford and Preston Waterflood Units, Spraberry Trend, West Texas," Report of Investigation No. 171, Bureau of Economic Geology, The University of Texas, Austin, 1988.
3. Lorenz, John: "Summary of Observations and Interim Interpretations: Fractures in Horizontal Spraberry Cores, E.T. O'Daniel Well #28", Internal Memo to Project Team, December 12, 1996.

Table 1
Fracture Orientation

Fracture Set	Average Strike (deg)	Total Range of Strikes (deg)
NNE	32	20-45
NE	43	35-50
ENE	70	50-85

Table 2
Fracture Spacing

Fracture Set	Spacing Range (ft)	Average Spacing (ft)
NNE	0.05-4.50	1.62
NE	0.73-5.75	3.17
ENE	0.04-13.0	3.79

Table 3
Diagenetic Events Affecting
1U and 5U Spraberry Fractures

1U Fractures	5U Fractures
- fracture formation	- fracture formation (NNE)
- minor dolomite in fractures	- calcite mineralization
- quartz mineralization	- barite mineralization
- barite mineralization	- fracture formation (ENE)
	- minor dolomite in fractures
	- quartz mineralization

Table 4
Comparison of Horizontal Cores Taken from the 1U Zone in the E.T. O'Daniel #28

Core Run No. (see Fig. 1.9)	Porosity	Oil Fluorescence	Permeability (md)	Water	Oil
#1	< 0.07	No	< 0.1	High	No
#2	< 0.07	No	< 0.1	High	No
#3	> 0.07	Strong	> 0.1	< 0.20	< 0.15
#4	> 0.07	Strong	> 0.1	< 0.20	< 0.15
#5	< 0.07	No	< 0.1	High	No
#6	< 0.07	No	< 0.1	High	No
#7	> 0.07	Strong	> 0.1	< 0.20	> 0.10
#8	> 0.07	Strong	> 0.1	< 0.20	> 0.10
#9	< 0.07	No	< 0.1	High	No

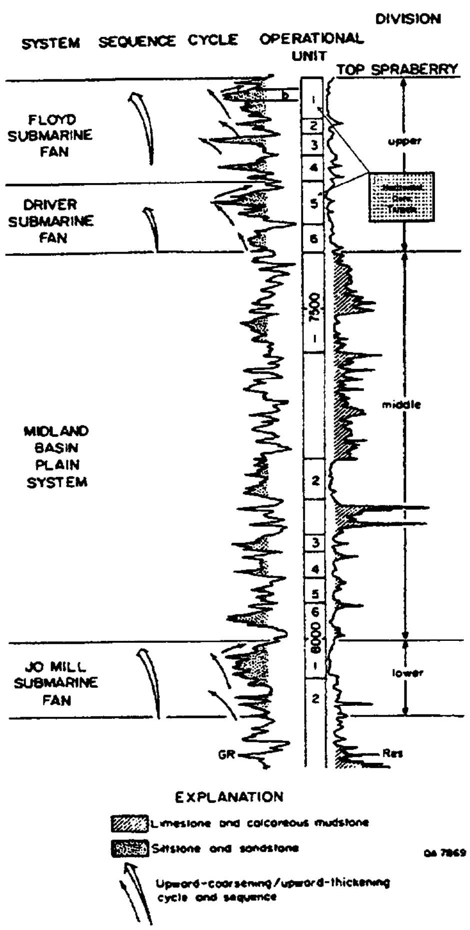

Figure 1 - Division of the Spraberry Formation in the central trend area, TXL Fee "B" No. 1 Well

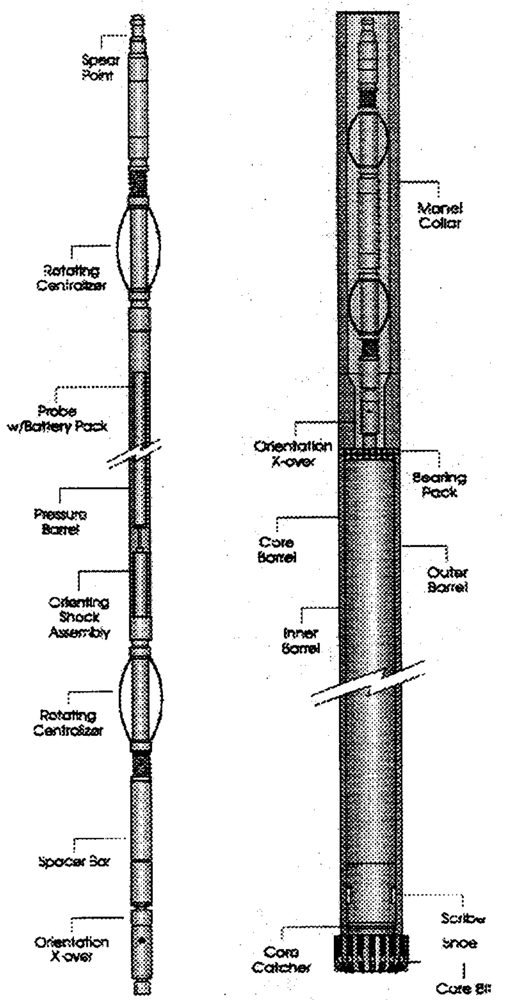

Figure 2 - Bottom hole coring and orientation assembly for horizontal coring of E.T. O'Daniel #28

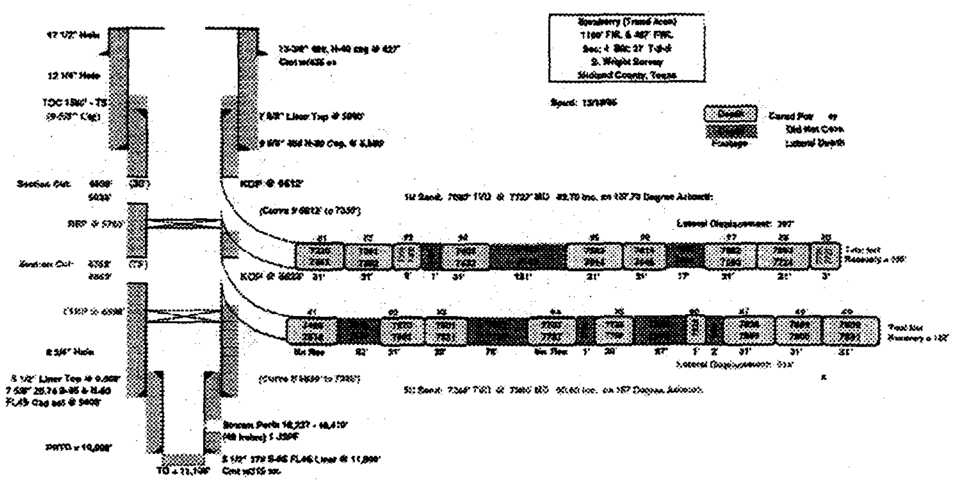

Figure 3 - E.T. O'Daniel #28

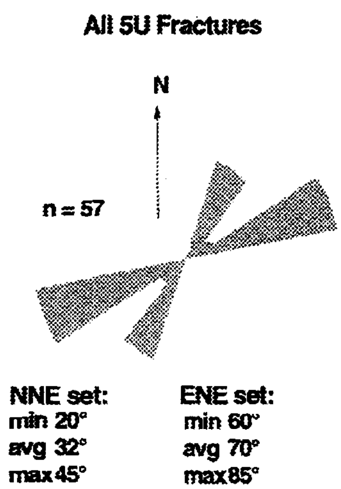

Figure 4 - Orientation of fractures in the 5U reservoir

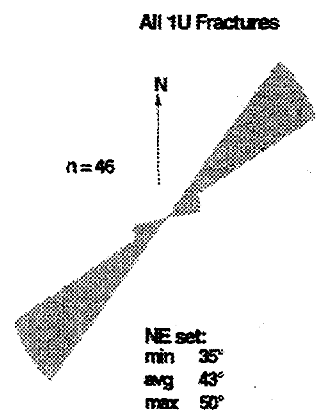

Figure 5 - Orientation of fractures in the 1U reservoir

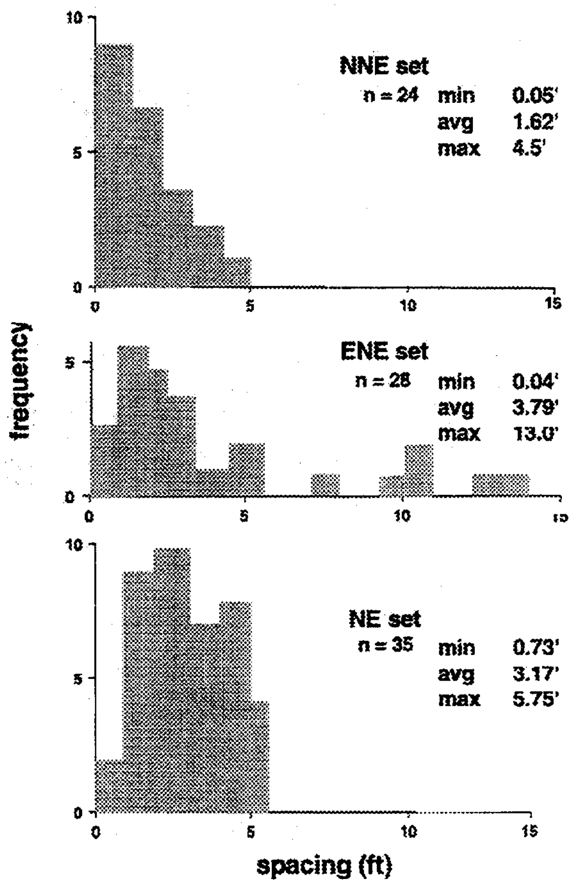

Figure 6 - Distribution of fracture spacing

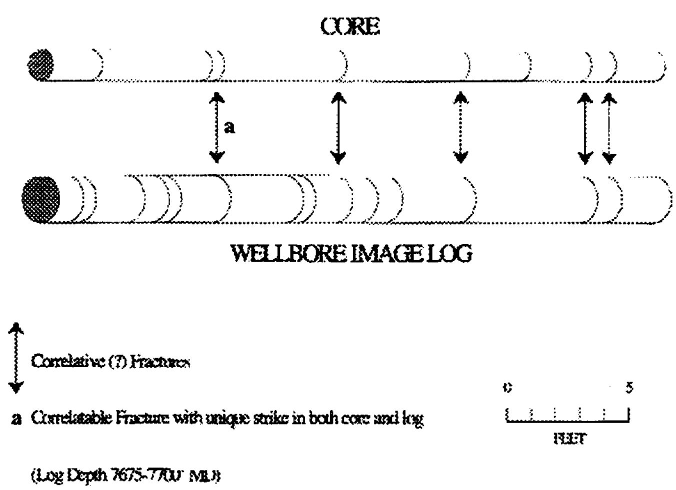

Figure 7 - Correlation between core fracture
and wellbore image log fracture

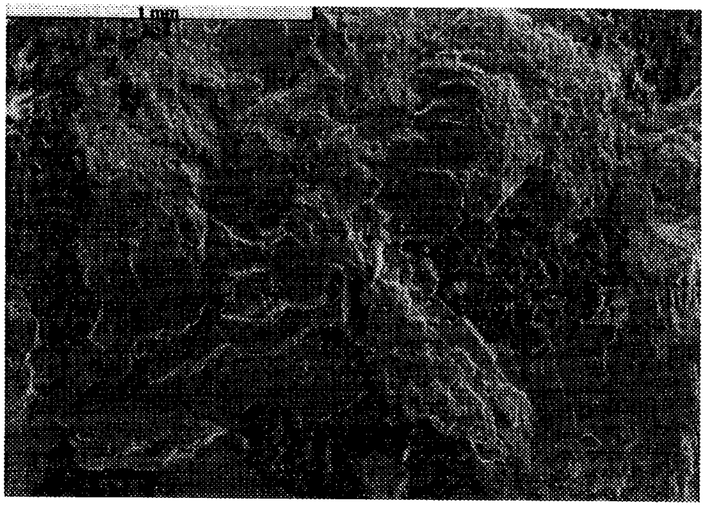

Figure 8 - SEM photomicrograph of barite that is covering the surface of a 1U fracture. Barite is the lighter gray mineral that forms the smooth surfaces and crystals. Note how it covers most of the microporosity at the fracture surface.

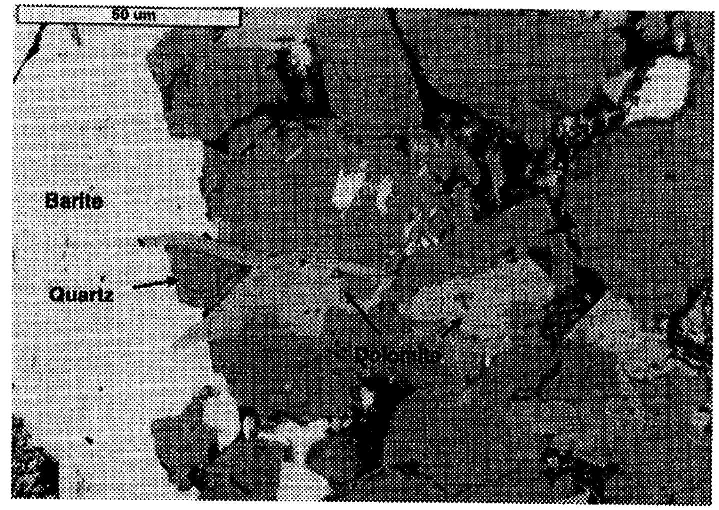

Figure 9 - SEM photomicrograph of a thin section across a 1U fracture. Photo shows various authigenic mineral phases including quartz, barite, and dolomite. The lighter gray mineral phases associated with the dolomite grains are ankerite (lightest gray) and ferroan dolomite (intermediate gray).

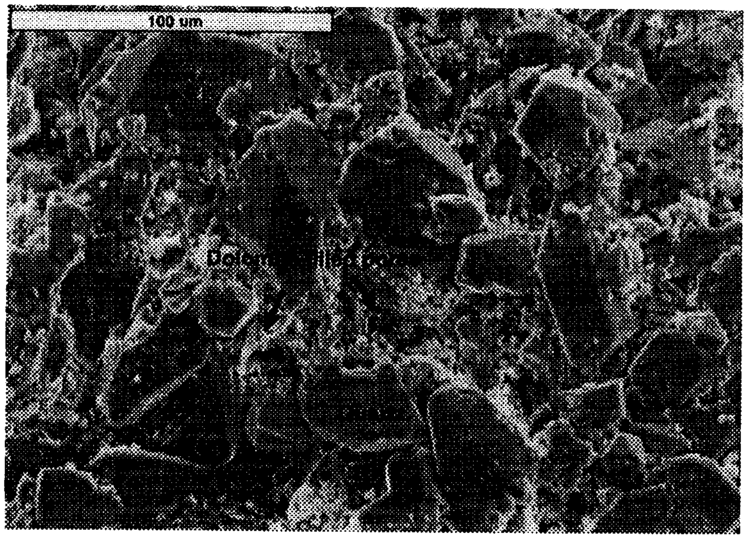

Figure 10 - SEM photomicrograph of a fracture surface from a 1U fracture. This surface has abundant quartz and dolomite mineralization, and dolomite has filled much of the intergranular pore space in this sample.

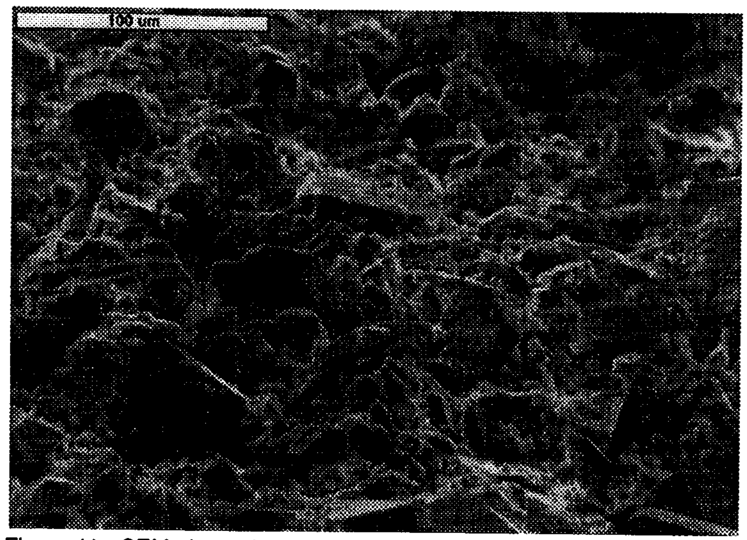

Figure 11 - SEM photomicrograph of a fracture surface from a 1U fracture. This oblique view shows that quartz crystals, although small, provide significant surface asperities to help keep fracture porosity open at depth.

Figure 12 - SEM photomicrograph of a fracture surface from a 5U fracture. This fracture surface appears to be unmineralized when examined at this magnification.

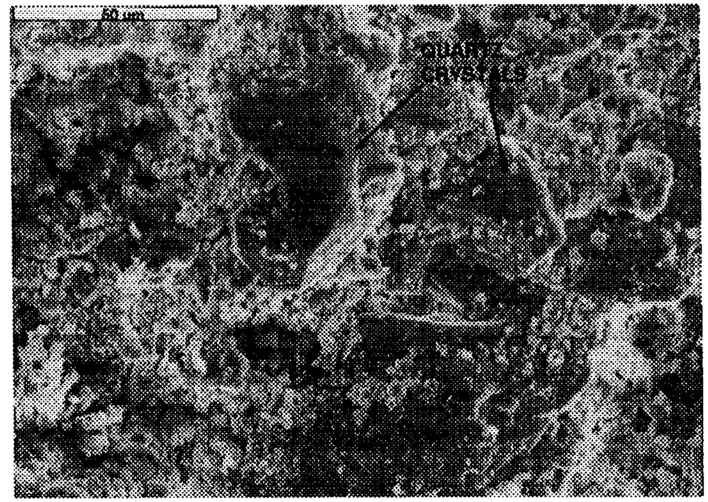

Figure 13 - SEM photomicrograph of the same surface in Figure 12. Note the presence of numerous euhedrally-terminated quartz crystals, indicating growth of the quartz minerals into the open space of the fracture. Euhedral quartz was seen on many 5U fracture surfaces when they were examined in SEM.

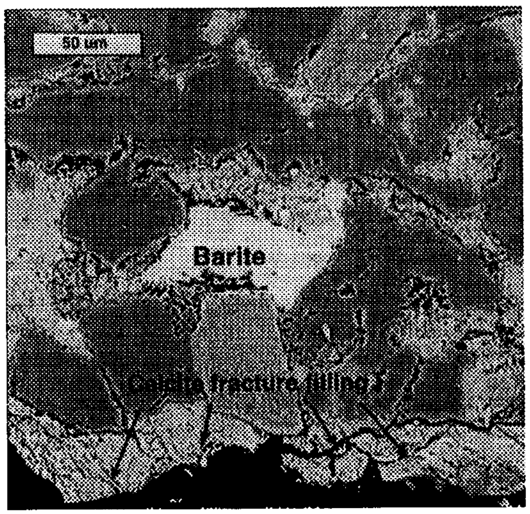

Figure 14 - SEM backscattered electron image of a polished thin section that was made perpendicular to a 5U fracture surface. This sample contains barite as a pore-filling mineral, and calcite as a fracture-filling phase. Calcite was also more abundant in pores near the fractures, and the calcite-filled fractures cut through previous diagenetic phases of carbonate that were present in the matrix, indicating formation after these phases were precipitated.

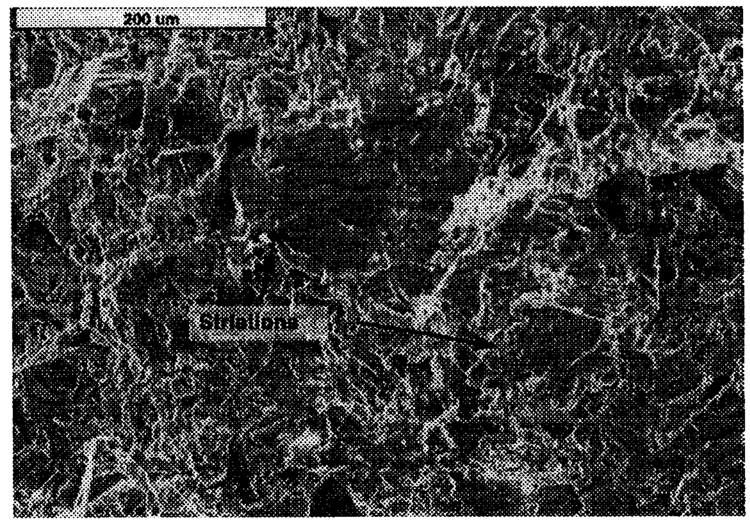

Figure 15 - SEM photomicrograph of the surface of a calcite-filled 5U fracture. Note the presence of striations on many crystal surfaces. These are believed to be due to dissolution along calcite twin plane lamellae.

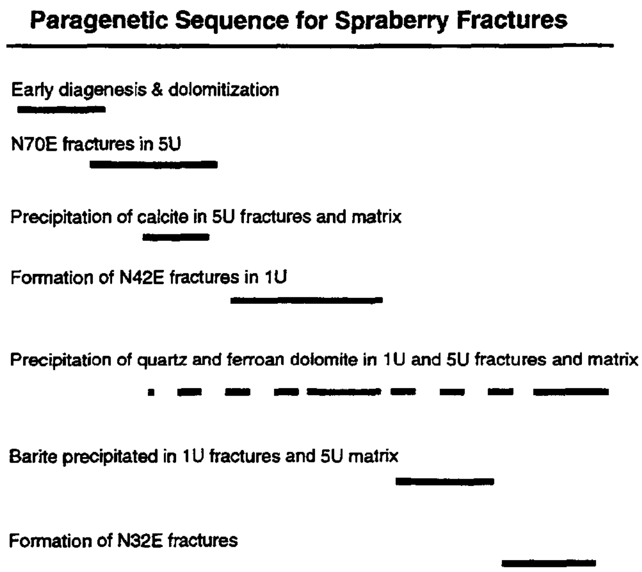

Figure 16 - Schematic showing the relative timing of various diagenetic events that occurred in Spraberry fractures.

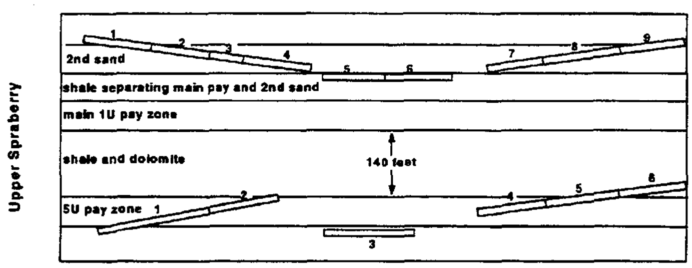

Figure 17 - Schematic diagram of the horizontal cores from the E.T. O'Daniel #28 well (not to scale).

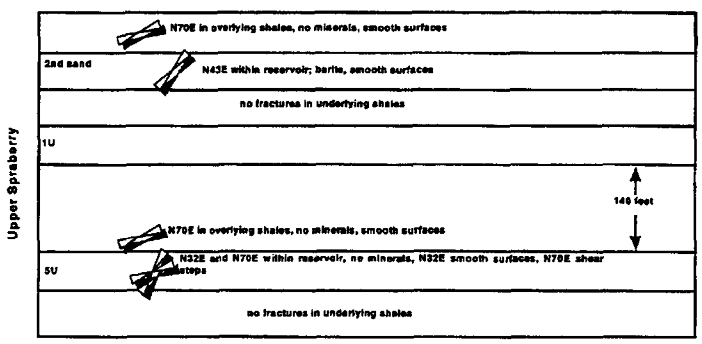

Figure 18 - Summary of fracture characteristics noted in the two horizontal cores from the E.T. O'Daniel #28 well for both pay and non-pay lithologies.

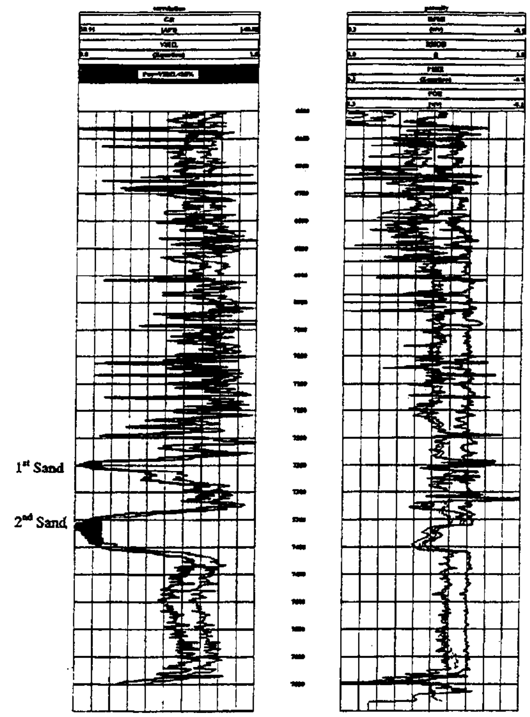

Figure 19 - Open-hole logs from the 1U zone in the horizontal well E.T. O'Daniel #28

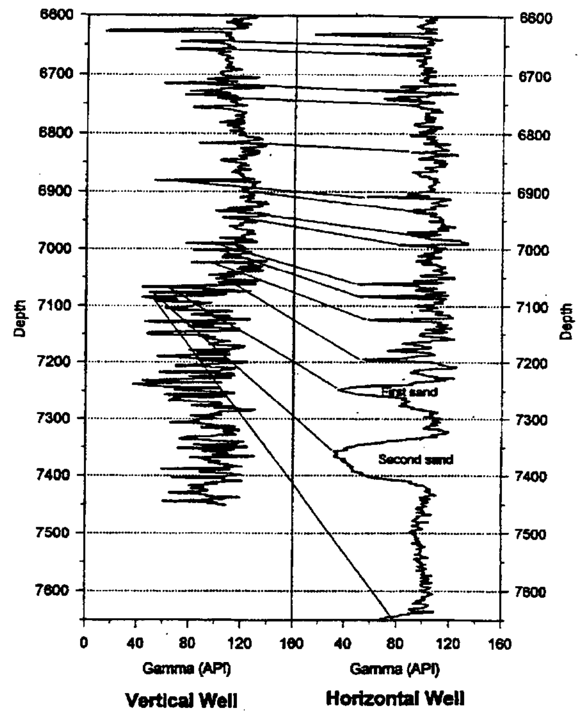

Figure 20 - Comparison of gamma ray log from vertical and horizontal logs in the E.T. O'Daniel #28 well. Note how individual beds appear to get thicker and more separated from each other as the curvature of the horizontal bore increases and approaches a horizontal line. Lines match various peaks within the Clearfork and demonstrate that the cored interval was not the main 1U pay zone but the sand immediately above

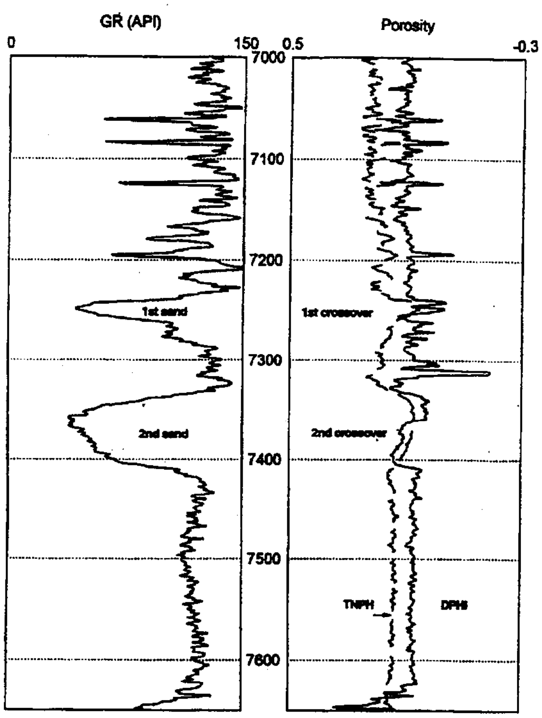

Figure 21 - Lithodensity/Neutron crossover log. This log shows only two pay zones, neither of which is as thick as the 1U was estimated to be in this area. The two minor pay zones correspond to the first and second sand above the 1U pay.

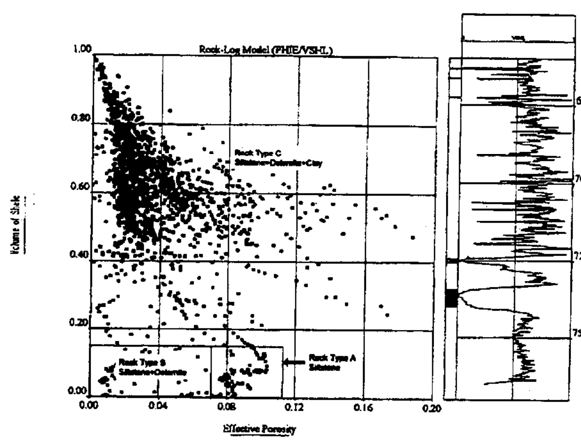

Figure 22 - Crossplot of volume of shale vs. effective porosity. Note that a relatively small amount of zones intersected by the horizontal well bore are classified as Rock Type A. good reservoir rock. Most of the horizontal cores have been observed to be Rock Types B and C.